doi.org/10.36721/PJPS.2026.39.9.252.1

Liposomal nanoparticle-encapsulated polyphenolic vitamins activate ferroptosis in glioma cells by suppressing the EGFR/NOTCH1/Hes1 pathway

Zhao Gao[1#], Yuxin Wang[2#], Shichao Su[2] and Jiayu Liu[1*]
[1]Department of Neurosurgery, Chinese PLA General Hospital, Beijing 100853, China
[2]Medical School of Chinese PLA, Beijing 100853, China

Abstract: **Background**: Vitamin phenol has anti-glioma potential but low bioavailability. Liposomal nanoparticles are effective drug delivery systems. Whether vitamin phenol-encapsulated liposomal nanoparticles can regulate ferroptosis in glioma cells remains unknown. **Objectives**: This study aims to investigate the role of polyphenolic vitamins-encapsulated liposomal nanoparticles in ferroptosis in glioma cells. **Methods**: LNP-Vig nanoparticles were prepared. U87MG cells were divided into control, LNP and LNP-Vig groups, with the latter receiving additional treatments (si-EGFR, pc-DNA EGFR, si-Hes1, or pc-DNA Hes1). Levels of ferroptosis, apoptosis and related proteins (EGFR/Hes1) were then detected. **Results**: The successfully formulated LNP-Vig nanoparticles induced ferroptosis and suppressed EGFR expression in U87MG cells, leading to increased apoptosis upon prolonged incubation. While si-EGFR reduced EGFR mRNA, the pc-DNA EGFR counteracted LNP-Vig's suppression of EGFR. The consistent changes in downstream NOTCH1 and Hes1 mRNA levels confirmed that LNP-Vig influences the NOTCH1/Hes1 pathway via EGFR inhibition. Both NOTCH1 blockade and Hes1 knockdown reduced the levels of ferroptosis-related proteins, whereas NOTCH1 activation or Hes1 overexpression inhibited ferroptosis (P<0.05). **Conclusion**: LNP-Vig promotes apoptosis by activating ferroptosis, an effect crucially dependent on Hes1 suppression. By modulating the EGFR/NOTCH1 pathway, LNP-Vig promotes ferroptosis in U87MG cells, thus identifying a potential new target for cancer treatment.

Keywords: EGFR; Ferroptosis; Glioma; Hes1; Liposomal nanoparticles; Polyphenolic vitamins

Submitted on 03-12-2024 – Revised on 09-10-2025 – Accepted on 19-10-2025

INTRODUCTION

polyphenolic vitamins has a variety of biological activities such as anti-oxidation, anti-inflammation and anti-tumor (Fig. 1) (Iervolino *et al*., 2021) and its application in the field of tumors has been widely studied. Although the use of polyphenolic vitamins in cancer treatment is still in its early stages, some studies have shown that it may inhibit tumor growth and have potential for cancer prevention. Emerging evidence suggests that polyphenolic vitamins may regulate tumor-related signaling pathways, including Wnt, PI3K-Akt and MAPK, via modulating miRNA expression (Das *et al*., 2022). Notably, however, its role in glioma research has not yet been extensively investigated.

polyphenolic vitamins may affect Wnt signaling pathway by regulating the expression of Axin (Husain *et al*., 2024). It promotes the proteolytic degradation of β-catenin (Wu *et al*., 2021, Agunloye *et al*., 2025), facilitating its rapid removal from the cell. This reduction in intracellular accumulation regulates β-catenin stability and consequently inhibits the Wnt signaling pathway. Another study found that phenol inhibited β-catenin phosphorylation, hindered its entry into the complex, thereby increasing its stability and promoting its accumulation in the nucleus (Wang *et al*., 2023). In regulating tumor biological behavior, phenol can modulate the expression or kinase activity of PI3K and the phosphorylation state of Akt, thereby affecting the PI3K-Akt signaling pathway (Ding *et al*., 2024). These findings collectively indicate the considerable potential of polyphenolic vitamins in oncology. Nevertheless, current research remains largely confined to basic science and the mechanisms underlying its diverse effects on miRNA expression are likely complex and multifactorial.

In recent years, studies have found that phenol has potential as an anti-cancer agent, including effects on glioma cells. Some studies suggest that phenolic vitamin compounds may affect EGFR activity by regulating EGFR phosphorylation or other downstream factors (Nag *et al*., 2020), but research on glioma is still in its infancy. Glioma is a primary brain tumor and iron plays an important role in tumor growth and metastasis (Tabu and Taga, 2022), because tumor cells have a high demand for iron to maintain their rapid growth and proliferation. However, iron may also cause oxidative stress, leading to oxidative damage and cell death (Chen *et al*., 2023). The mechanism of action of polyphenolic vitamins in tumors may involve iron regulation. However, due to the low bioavailability and instability of polyphenolic vitamins (Vesely *et al*., 2021), its use in glioma treatment is limited. Therefore, it is urgent and necessary to develop new carrier delivery technology.

**Corresponding author:* e-mail: liujiayu@pku.edu.cn
#These authors contributed equally and are the co-first authors.

Nanotechnology is an emerging drug delivery technology that can improve the bioavailability of drugs (McClements and Ozturk, 2022) and enhance the accumulation of drugs in tumor tissues, thereby improving the efficacy of drug therapy. Liposome nanoparticles have been widely used in cancer therapy as a common nanocarrier (Seidu *et al*., 2022). Benefiting from good biocompatibility, stability and drug loading capacity, liposomes can effectively encapsulate and deliver drugs such as polyphenolic vitamins.

In this study, the regulation of the Hes1 gene (downstream of the EGFR pathway) by polyphenolic vitamin-encapsulated liposomal nanoparticles was investigated, and its mechanism of action in ferroptosis of glioma cells was further explored. Cell experiments were conducted to study the effects of this treatment strategy on glioma cell proliferation, apoptosis, and ferroptosis, thereby laying a foundation for the future development of efficient therapeutic strategies with low side effects. At the same time, the potential mechanism of polyphenolic vitamins and liposomal nanoparticles in the treatment of glioma is expected to be further elucidated, providing a new theoretical and practical basis for the application of nanotechnology in cancer treatment.

MATERIALS AND METHODS

Materials

Vitamin polyphenols (batch number: 84650-60-2; Purity: 99%; Bought in Shanghai Xuanya; Vitamins were extracted from green tea, grape seeds, etc., which can not only resist inflammation and oxidation but can also reduce blood lipid and blood pressure to prevent cardiovascular diseases. The plant map is shown in Fig. 2. Human glioblastoma cell line U87MG cells (Shanghai Huzhen Industrial Co., Ltd.); NOTCH1 pathway agonist DLL4, NOTCH1 pathway γ-Secretase inhibitor (Beijing Biolab); monoclonal antibody, IgG secondary antibody (UK Abcam company); RPMI-1640 medium (Guangdong Huankai Microbial Technology Co., Ltd.); cell lysate (Shanghai Lianmai Biotechnology); protease inhibitors (Shanghai Yisheng Biotechnology); fetal bovine serum (Qingdao Yusen Biotechnology); RT- PCR reverse transcription kit (Shanghai Jiachu Biotechnology); TRIzol reagent and fluorescence quantitative kit (Chengdu Huaxia Chemical Reagent Co., Ltd.); Transwell chamber (Beijing Unicom Biotechnology); CCK-8 kit, cDNA synthesis kit (Beijing Tiangen Biochemical). TEM instrument model: JEM2100 (80KV by default).

Preparation of LNP-Vig

Selected phospholipids and solvent were mixed and stirred according to a certain ratio, so that lipids formed liposomes in the solvent. Polyphenolic vitamins was encapsulated into liposomal nanoparticles via dropwise addition of its solution to the liposome suspension under stirring or ultrasonication. Polyethylene glycol (PEG) was added to increase the stability and biocompatibility of the liposomal nanoparticles, followed by centrifuge to remove unencapsulated vitaminol and other by-products and then washing the nanoparticles with an appropriate solution. 10 mg of LNP-Vig polymer was then dissolved in 10 ml of UP water, followed by stirring at room temperature for 6-8 hours until completely dissolved, sonicating for 0.5 hours and passing it through a 0.45 μm filter membrane to obtain LNP-Vig nanoparticles. The encapsulation efficiency of polyphenolic vitamins was determined to be 85.3% using the ultracentrifugation-HPLC method (Dong *et al*., 2011). *In vitro* release experiments demonstrated that LNP-Vig achieved a cumulative release rate of 78.5% in PBS over 72 hours, indicating sustained-release characteristics.

Characterization of LNP-Vig

The Zeta potential of LNP-Vig was measured by a particle size analyzer.The nanoparticle solution was diluted, ultrasonicated, and then added dropwise onto aluminum foil. After drying at room temperature, the sample was gold -sputtered and observed under a transmission electron microscope (JEM2100). Deionized water was added into the sample prior to TEM microscopy. Following ultrasonic treatment, the sample was filtered twice through a membrane filter and then applied to a carbon support film, where it was allowed to air-dry. Then phosphotungstic acid was added, dried at room temperature, imaged by electron microscope at 80-120kv, followed by observation of the sample under transmission electron microscope and image analysis (Zhang *et al*., 2023).

Cell culture, grouping and transfection

All cells were cultured in RPMI-1640 medium, added with 10% fetal bovine serum, placed in an incubator and the environment was controlled at 37°C and 5% CO2. Growth of the cells was observed and culture medium was replaced on time. When the confluence of the cells was 80%, the cells were trypsinized and passaged (Yathindranath *et al*., 2022).

U87MG cells were divided into 3 groups as follows: control group, LNP group and LNP-Vig group. At the same time, the LNP-Vig group was divided into LNP-Vig+si-EGFR group, LNP-Vig+pc-DNA EGFR group, LNP-Vig+si Hes1 group and LNP-Vig+pc DNA Hes1 group. The control group was cultured with 50% PBS for 48h. At 24 hours post-transfection, observation under a fluorescence microscope was conducted. If the proportion of cells displaying green fluorescence in the field of view exceeded 80%, the transfection procedure was deemed effective and suitable for subsequent experiments.

The human glioblastoma cell line U87MG used in this study was purchased from Shanghai Huzhen Industrial Co., Ltd. (Shanghai, China). This cell line is a commercial product with anonymized origin, and no additional informed consent was required. The study protocol was approved by the Ethics Committee of Chinese PLA General Hospital (Approval No.: S2022-763-01).

Table 1: Real-time PCR primers and primer sequences.

EGFR	5'-GGCACAGTGTGTCCAAATGTG-3	5'-AGGAAGCTGCTCTGTGTTCC-3'
NOTCH1	5'-GCCAGTGTCCATGTGTGTGA-3'	5'-GTCATGGGACGAGGAGTTGT-3'
HES1	5'-GGTGGAGACGGAGGAGTTG-3'	5'-AGAGAGCCGGAGACAGAACT-3'

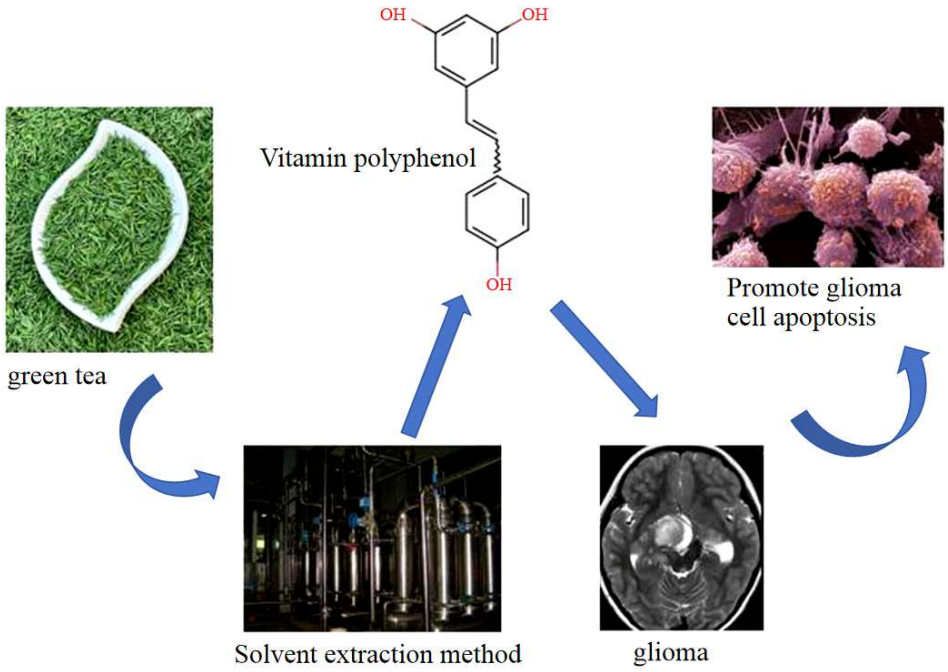

Fig. 1: Extraction process and research ideas for vitamin polyphenols.

Fig. 2: Plant diagram of green tea.

Assessment of blank nanoparticle cytotoxicity

To evaluate the biocompatibility of the blank lipid nanoparticle (LNP) carrier itself, the CCK-8 assay was used to detect its impact on U87MG cell viability. Briefly, U87MG cells were seeded in a 96-well plate at a density of 5×10^3 cells per well. After cell adhesion, the medium was replaced with fresh medium containing different concentrations of blank LNPs (equivalent to the carrier concentrations used in the LNP-Vig groups). Following further incubation for 24 and 48 hours, 10 μL of CCK-8 solution was added to each well and the plate was incubated at 37°C for 2 hours. The absorbance (OD value) of each well was measured at a wavelength of 450 nm using a microplate reader. Cell viability was calculated using the formula: (OD value of experimental group - OD value of blank well) / (OD value of control group - OD value of blank well) × 100%. The experiment was independently repeated three times.

Flow cytometry was used to detect apoptosis in cells

After cells from each group were digested, they were made into a suspension of 1×106ml, centrifuged and washed with PBS and resuspended. 150μl of buffer was then added with Annexin V-FITC (10μl) and PI staining solution (5μl) and protected from light. After incubation for 15 min, cell apoptosis was observed by flow cytometry (Del Re *et al*., 2014).

Real-time PCR detection of gene expression

RNA was extracted from U87MG cells by TRIzol method and it was reverse transcribed into cDNA by TaqManTM

advanced miRNA cDNA synthesis tool. RT-qPCR was performed using SYBR fluorescent PCR technology. Analysis was performed using real-time PCR system. Relative levels were estimated using 2−ΔΔCt method (Livak and Schmittgen, 2001). All primers used (sequences are listed in table 1) were validated for amplification efficiency using the standard curve method. The cDNA template was serially diluted (e.g., in 5-fold dilution steps) and qPCR reactions were performed. The amplification efficiencies of all primers fell within the range of 90%–110%, with correlation coefficients (R^2) greater than 0.99, meeting the requirements for reliable quantification. Following each qPCR run, melting curve analysis was conducted to confirm the specificity of the amplified products. All reactions exhibited a single sharp peak, indicating that amplification produced a single specific product without nonspecific amplification or primer-dimer formation.

Western blot

The total protein of U87MG cells was extracted with TriZol reagent and its concentration was detected. The electrophoresed total protein was heated to 100°C and incubated for 5 minutes and then electrophoresed using SDS-polyacrylamide gel (120 V, 100 minutes). The separated proteins were then transferred to PVDF membranes. After blocking with 5% skim milk, the membrane was incubated with Akt antibody, EGFR antibody, TF antibody, TFR antibody and GAPDH overnight at 4°C. The next day, the samples were incubated and the membrane was washed 3 times and incubated with secondary antibody (1:10,000) for 1 hour (37°C). After washing three times with PBS, the Western blot bands were analyzed for optical density using ImageJ, with GAPDH as the internal reference for normalization. The experiment was independently repeated three times and the results are expressed as mean ± standard deviation (Mijiti *et al*., 2023).

Detection of reactive oxygen species (ROS) by DCFH-DA method

After cells grew to an appropriate density, the stock solution of DCFH-DA (2',7'-dichlorodifluorofluorescein acetate) was diluted to an appropriate concentration with an appropriate solvent (DMSO). After washing, an appropriate amount of diluted DCFH-DA staining solution was added to fully cover the cells, followed by incubation at 37°C for 1 hour. The samples were washed with PBS 3 times, centrifuged toremove PBS and then ROS was detected by flow cytometry (Bode *et al*., 2020).

Detection of malondialdehyde (MDA) by thiobarbituric acid method

Cell lysis solution (such as RIPA buffer) lysed the cell membrane and released MDA from the cell. Cell lysate was obtained by adding thiobarbituric acid (TBA) reagent after mixing, followed by the addition of phosphate buffer to keep the sample pH at 2-3. The sample was heated and reacted in a water bath, usually at 95°C for 20-30 minutes, to promote the reaction of MDA and TBA to generate a stable pigment. The sample was cooled and centrifuged to remove the precipitate. Detection of the absorbance of the pigment was performed at a wavelength of 532 nm (Jiang *et al*., 2022).

Observation of ROS by confocal microscope

The 2',7'-dichlorofluorodiacetate (DCFH-DA) fluorescent probe was added to the culture medium and the fluorescent probe was passed through the cell membrane into the cell and incubated for 30 minutes, followed by washing to remove excess DCFH-DA. On the confocal microscope stage, the appropriate excitation wavelength was selected, followed by fluorescence detection at the desired wavelength (Yu *et al*., 2023).

Statistical analysis

All experimental data were analyzed using SPSS21.0 and GraphPad Prism software. Measurement data were shown as mean ± SD and assessed by T/F test. $P<0.05$ was considered a significant difference.

RESULTS

Preparation of LNP-Vig and its pro-apoptotic effect on glioma cells

The LNP-Vig nanoparticles were successfully prepared and their morphology was observed by transmission electron microscopy (JEM2100) (Fig. 3A). The results showed that the LNP-Vig nanoparticles had an average particle size of 38.65 nm and a polydispersity index (PDI) of 0.021. The nanoparticles formed a regular round shape without aggregation and exhibited good dispersion (Fig. 3B). The zeta potential was -54.5 mV, indicating a homogeneous particle distribution and good stability (Fig. 3C). CCK-8 assay results demonstrated that, at concentrations equivalent to those used in the LNP-Vig experimental groups, treatment with blank LNPs for 24 and 48 hours did not significantly affect the viability of U87MG cells (vs. the control group, $P>0.05$, Fig. 3D). And when used in U87MG cell culture, it was found that, the apoptosis rate increased with prolonged culture time for LNP-Vig nanoparticles (vs the control group, $P<0.05$, Fig. 3E).

LNP-Vig activates glioma cell ferroptosis via EGFR pathway

To further analyze the anticancer effect of LNP-PV on U87MG cells, Western blot and colorimetric assays were performed. It was found that both PV and LNP-PV promoted increased expression of ferroptosis-related proteins, including TF and TFR, in U87MG cells (Figs. 4A – C). Notably, the effect of LNP-PV was the most prominent (vs. PV group, $P<0.05$, Figs. 4F – G). To explore whether this phenomenon was associated with ferroptosis, confocal microscopy was performed to observe intracellular ROS levels in U87MG cells.

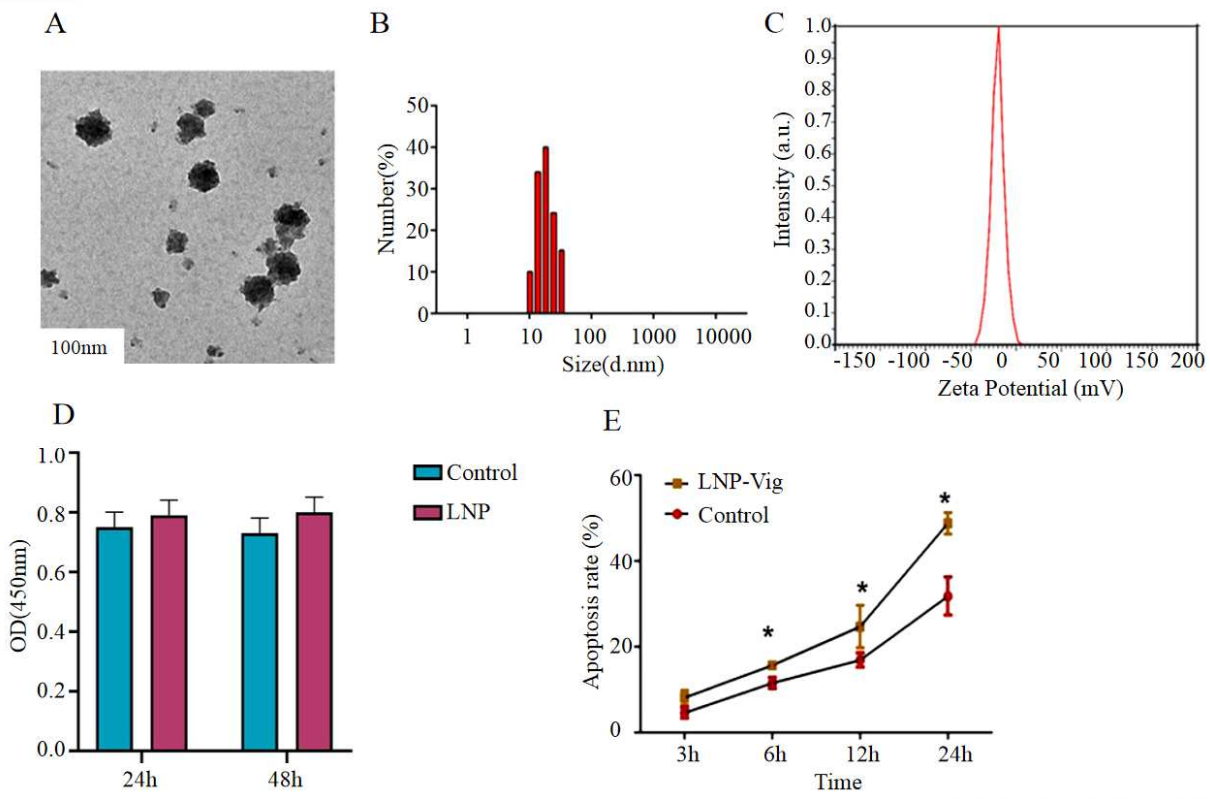

Fig. 3: Preparation of LNP-Vig and its pro-apoptotic effect on glioma cells.
Note: (A) Electron micrograph (×200um); (B) Size distribution; (C) Zeta potential; (D) Viability after blank LNP treatment; (E) Apoptosis rate of U87MG. *P<0.05.

The LNP-PV group exhibited the highest levels of non-oxidized ROS, forming dense green fluorescence (vs. other groups, P<0.05, Fig. 4E), followed by the PV group. These findings indicated that LNP-PV activated ferroptosis in U87MG cells, whereas EGFR protein expression showed the opposite trend (Fig. 4D). These results suggested that, the activation of U87MG ferroptosis by LNP-Vig may be related to EGFR.

LNP-Vig inhibits the EGFR pathway and affects downstream NOTCH1 pathway

To further analyze the mechanism by which LNP-PV affects ferroptosis, U87MG cells were transfected to inhibit or upregulate EGFR. The LNP-PV group exhibited an inhibitory effect on EGFR mRNA expression (Fig. 5A). Moreover, EGFR mRNA expression was greatly reduced after transfection with si-EGFR (vs. LNP-PV group, P<0.05), indicating that LNP-PV inhibited EGFR expression.The combined intervention of pc-DNA EGFR significantly reversed this phenomenon, which was higher than that of LNP-Vig group (vs LNP-Vig group, P<0.05) and its protein expression was also significantly increased (Fig. 5B) The expressions of downstream NOTCH1 mRNA and Hes1 mRNA were also regulated in a consistent direction (Figs. 5C, D), confirming that LNP-Vig inhibits the EGFR pathway and affects inhibition of NOTCH1 pathway and Hes1 gene.

LNP-Vig activates EGFR pathway and ferroptosis in glioma cells

On the basis of the previous experiments, it was further found that the expression levels of ferritin, TF, and TFR were increased in the LNP-PV and LNP-PV + si-EGFR groups (vs. the control group, P<0.05, Figs. 6A-C). In contrast, these protein expressions were significantly inhibited in the pc-DNA EGFR group (vs. other groups, P<0.05), and the levels of Fe2+ and ROS also showed consistent changes (Figs. 6D-G).

LNP-Vig inhibits NOTCH1 pathway, reduces Hes1 and plays the role of ferroptosis activation

A specific γ-secretase blocker of the NOTCH1 pathway and the agonist DLL4 were used, together with upregulation of the Hes1 gene and pc-DNA-mediated silencing, to analyze the changes in ferroptosis-related proteins in U87MG cells The results showed that, the expression of ferroptosis-related proteins was lower than that in the LNP-Vig group after blocking NOTCH1, while the si-Hes1 group had the same trend (P<0.05, Figs. 7A-I). After activating the NOTCH1 pathway or overexpressing Hes1, ferroptosis was reversed (P<0.05, Figs. 7A-I). It was confirmed that LNP-Vig promotes apoptosis of U87MG and activation of ferroptosis is inhibited by Hes1 to play a key role.

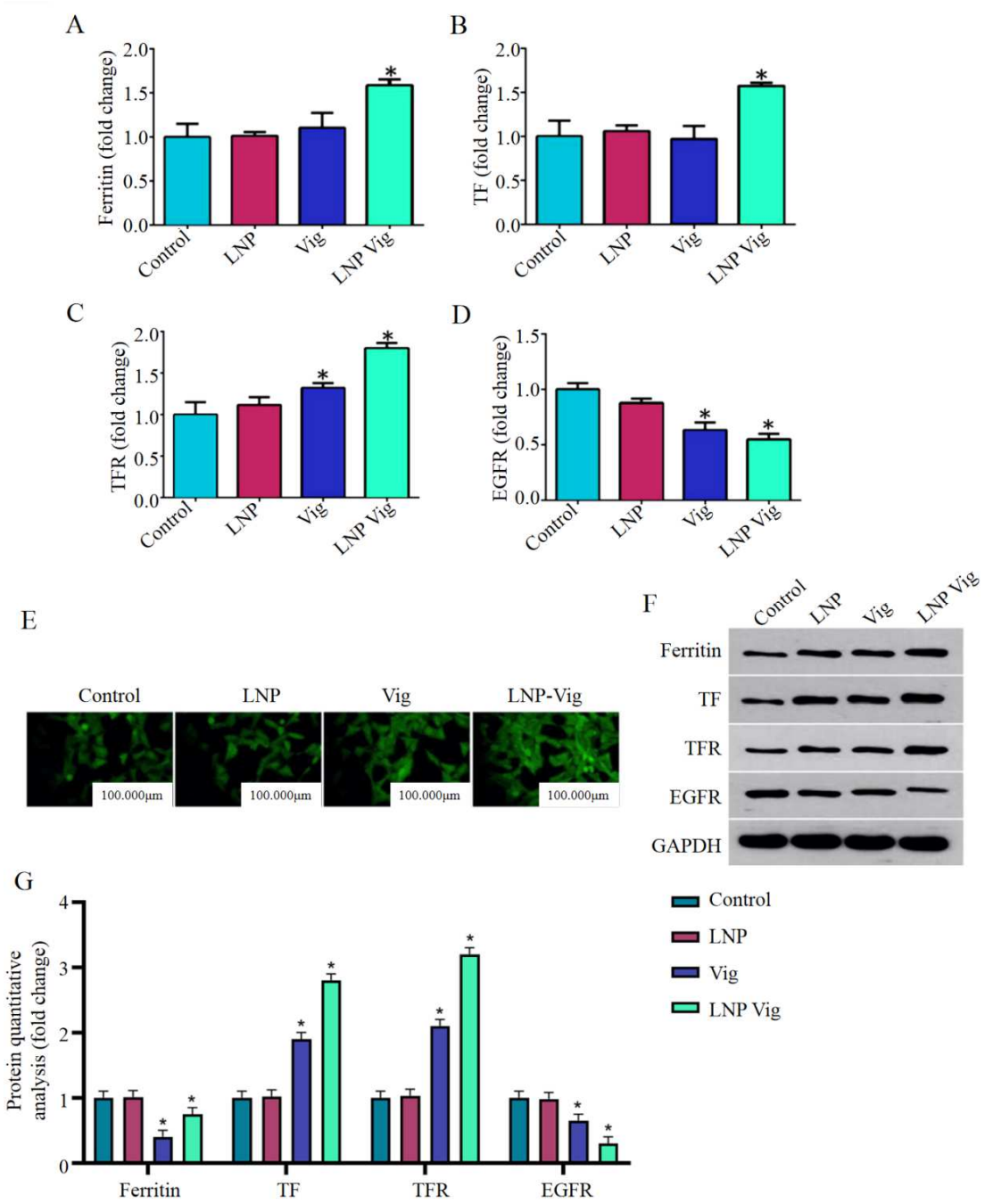

Fig. 4: LNP-Vig activation of glioma cell ferroptosis is related to EGFR pathway.
Note: (A): Ferritin expression; (B): TF expression; (C): TFR; (D): EGFR; (E): Confocal microscope observation of ROS; (F): Protein expression bands from each group; (G): Quantitative analysis of protein expression from each group, *P<0.05.

DISCUSSION

Ferroptosis is a recently discovered form of cell death (Ye *et al*., 2024) with significant value in tumor research. Different from traditional apoptosis and necrosis, it can be achieved by regulating intracellular iron metabolism as a non-apoptotic and non-necrotizing programmed cell death (Fan *et al*., 2022, Stockwell, 2022). Studies have shown that (Sacco *et al*., 2021, Liang and Ferrara, 2021), by interfering with balance of iron metabolism, it can lead to death of tumor cells, thereby inhibiting the growth and spread of tumors. Related molecules and proteins in the iron metabolic pathway become potential drug targets (Bu and Wang, 2025). Studying the regulatory mechanism of ferroptosis will help to discover new anti-tumor drugs and treatments.

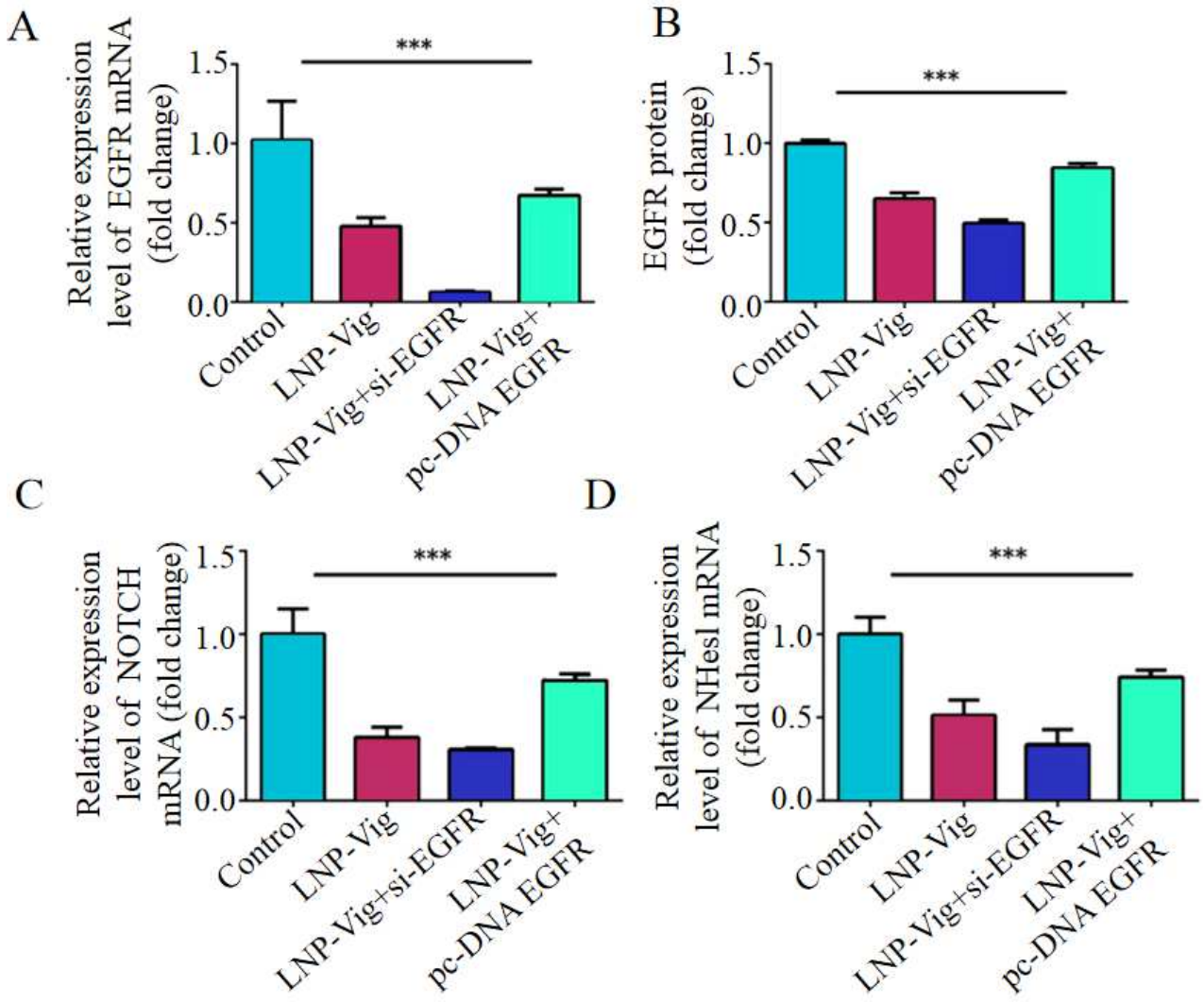

Fig. 5: LNP-Vig inhibits EGFR pathway, and inhibits NOTCH1 pathway gene, Hes1 gene.
Note: (A-B): Relative expression of EGFR mRNA and protein; (C): Relative expression of NOTCH1 mRNA; (D): Relative expression of Hes1 mRNA, ***P<0.05.

In this study, LNP-PV particles were successfully prepared and were found to exert a pro-apoptotic effect on glioma cells. To further explore the underlying mechanism, ferroptosis-related proteins were detected. It was found that both PV and LNP-PV promoted ferroptosis, with the effect of LNP-PV being more pronounced. This enhanced efficacy is likely attributable to the superior physicochemical properties of the LNP-Vig nanoformulation. As shown in the results, the successfully prepared LNP-Vig nanoparticles exhibited a regular spherical morphology. The uniform nanoscale size (low PDI) facilitates cellular uptake, while the appropriate zeta potential ensures good dispersibility and stability of the nanoparticles within the system, thereby laying the foundation for their long-circulating properties *in-vivo*. Furthermore, this study demonstrated that the blank LNP carrier, at equivalent concentrations, had no significant impact on cell viability. This finding rules out toxicity induced by the nanocarrier itself and further confirms that the observed pro-apoptotic and ferroptosis-inducing effects of LNP-Vig are primarily attributable to the encapsulated polyphenolic vitamins. More importantly, liposomal nanoparticles can protect polyphenolic vitamins from degradation in the external environment as drug carriers (Sweed *et al*., 2024), prolonging its existence time in the body and allowing more polyphenolic vitamins to enter cells, thereby enhancing its bioavailability and stability, which allows LNP-Vig to release polyphenolic vitamins more effectively and improve the antitumor effect of polyphenolic vitamins. This enabled more Vig to be delivered effectively to glioma cells, thereby explaining the increased ROS accumulation and ferroptosis activation observed in the LNP-Vig group. Studies have found that nanoparticles themselves can promote the production of ROS in cells and increased ROS is associated with ferroptosis (Wang *et al*., 2024).

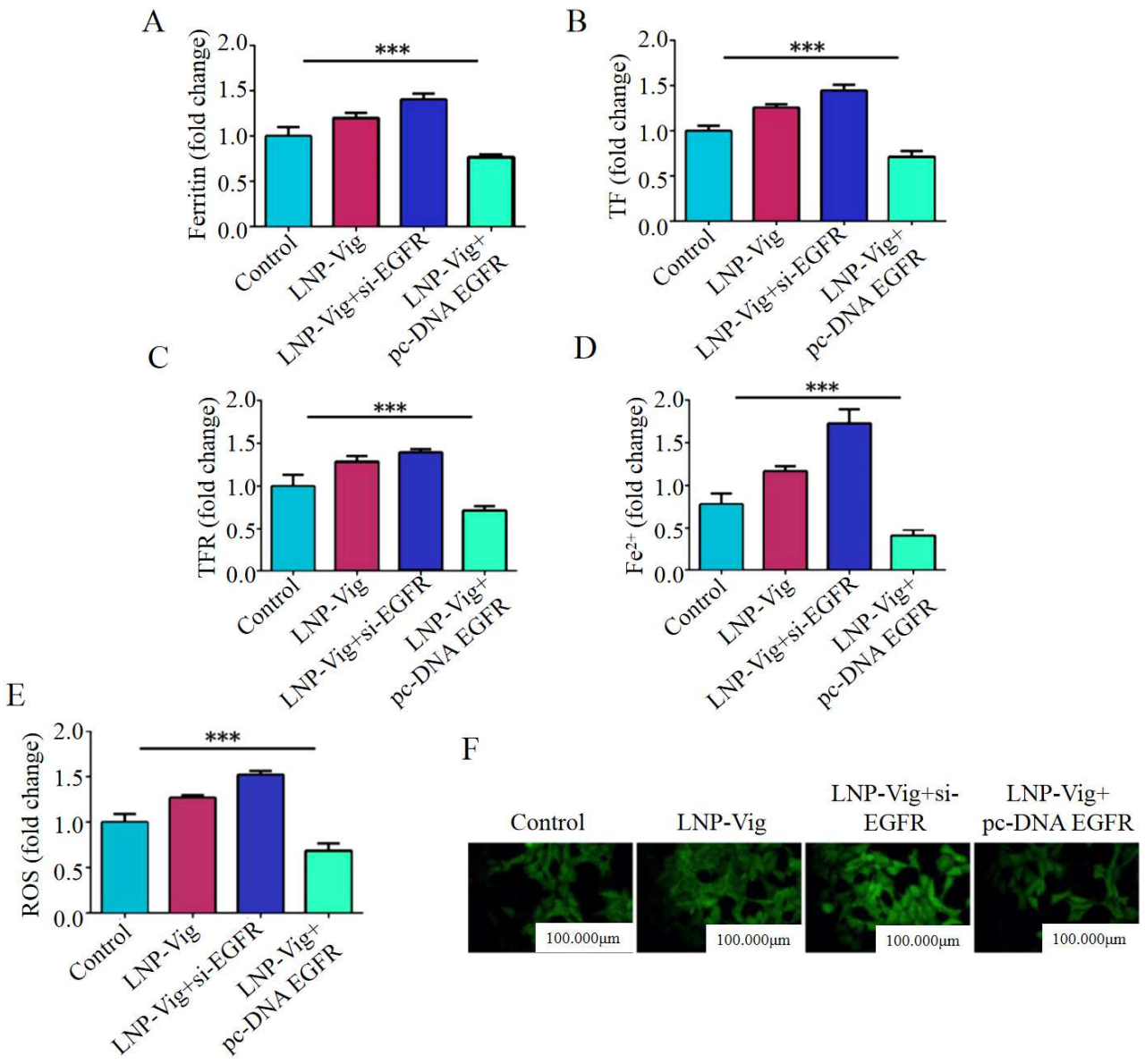

Fig. 6: LNP-Vig activates EGFR pathway to activate ferroptosis in glioma cells.
Note: (A): Ferritin expression;(B): TF expression; (C): TFR; (D): Fe2+ level; (E): ROS level; (F): Confocal microscope observation (×200), ***P<0.05.

It was also suggested by the study findings that increased ROS may be an important factor in promoting ferroptosis. The level of intracellular non-oxidized ROS in the LNP-Vig group was highest, suggesting that LNP-Vig may indirectly promote ferroptosis by increasing ROS production. The expression of EGFR protein in the NP-Vig group was relatively low, which may be a potential mechanism for LNP-Vig in promoting ferroptosis by inhibiting the EGFR pathway. The accumulation of iron ions in glioma cells can trigger cell death through various pathways. The most important of which is the iron-dependent death pathway, known as "ferroptosis" (Lu *et al*., 2021).

During ferroptosis, iron ions catalyze the generation of excessive hydroxyl radicals (ROS), leading to increased intracellular oxidative stress, cell membrane lipid peroxidation (Rochette *et al*., 2022), DNA damage, protein oxidation, etc. and tumor cell death. After treatment with LNP-PV, EGFR mRNA expression was significantly reduced, indicating that LNP-PV inhibited the transcription of the EGFR gene and subsequently suppressed the activity of the EGFR pathway. The results on further transfection of si-EGFR (siRNA that inhibits EGFR) showed that the interference of si-EGFR strengthened the inhibitory effect of LNP-Vig on EGFR gene and further reduced the activity of EGFR pathway.

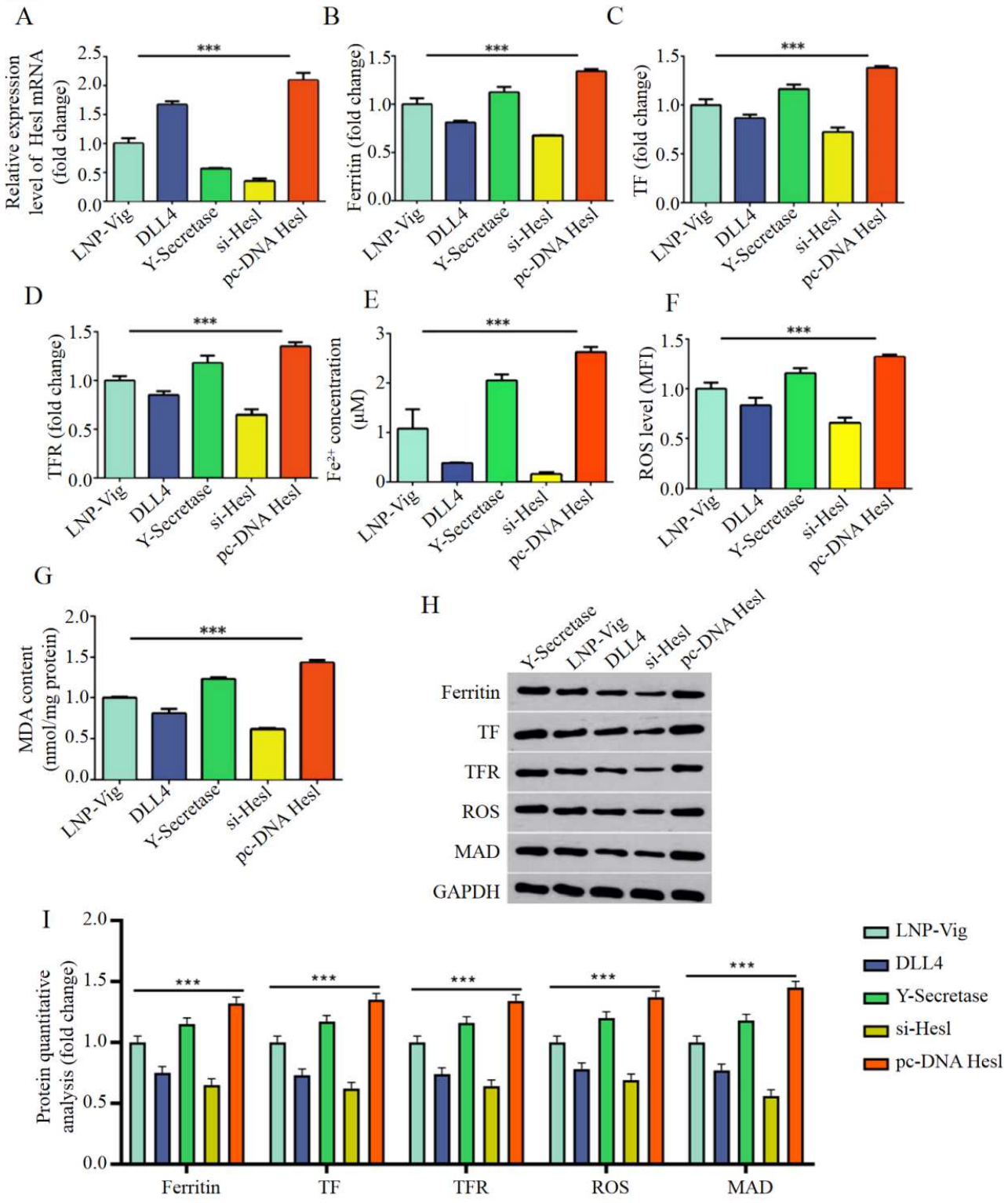

Fig. 7: LNP-Vig inhibits the NOTCH1 pathway and activates ferroptosis, which plays a key role in reducing Hes1 gene expression.

Note: (A) Hes1 mRNA relative expression; (B) Feritin expression; (C) TF expression; (D) TFR; (E) Fe2+ level (F) ROS level; (G) MAD expression; (H) Protein expression bands from each group; (I) Quantitative analysis of protein expression from each group, ***P<0.05.

pc-DNA EGFR can reverse the inhibitory effect of LNP-Vig on EGFR gene and increase the activity of EGFR pathway. After transfection with si-EGFR, the expression of EGFR mRNA was further reduced, which indicated that the inhibitory effect of LNP-Vig on EGFR might be enhanced through the interference of si-EGFR. As the main channel for iron uptake by cells, when the transferrin receptor is inhibited in EGFR pathway, TFR1 may be up-regulated, thereby increasing the uptake of iron by cells. When the EGFR pathway is inhibited, AKT activity may decrease, thereby inhibiting cell survival (Zhang *et al*., 2025; Imbastari *et al*., 2021). In addition, inhibition of the EGFR pathway may lead to decreased activity of MAPK pathway-related proteins such as ERK, JNK and p38, affecting cancer cell growth (Le and Fan, 2023). In this study, LNP-Vig treatment led to downregulation of NOTCH1 and Hes1 expression under EGFR pathway inhibition. However, after co-transfection of pc-DNA EGFR, this regulatory phenomenon was reversed and the expression levels for NOTCH1 and Hes1 genes were restored and increased. Therefore, it is speculated that the inhibitory effect of LNP-Vig may act through the NOTCH1 and Hes1 downstream pathways by regulating EGFR pathway gene expression. At the same time, iron ion (Fe2+) and intracellular ROS levels were also consistent with these protein expression changes. In conclusion, LNP-Vig nanoparticles inhibit EGFR expression, subsequently modulating the expression of ferroptosis-related proteins and promoting ferroptosis. These findings provide an important foundation for further exploring the mechanism of action of LNP-Vig in glioma cells and underscore the value of ferroptosis in oncology research.

Another study has shown (Yasinjan *et al*., 2023) that polyphenolic vitamins can inhibit excessive accumulation of iron ions in glioma cells, regulate transferrin, mouse ferritin, orange red protein and iron release protein HCP1, thereby alleviating oxidative stress and reducing the degree of cellular oxidative damage. Studies have also shown that polyphenolic vitamins can affect the balance and metabolism of iron in lung cancer cells by regulating iron ion transporters, iron metabolism enzymes and other factors.

In previous studies (Paskeh *et al*., 2024), polyphenolic vitamins may affect the level of free iron ions in cells by regulating iron ionophores such as iron-locked iron (LIP). In addition, it can also affect the Bcl-2 family, Caspase family and Atg family to promote cell apoptosis and autophagy and remove or utilize excess iron ions. In this study, EGFR mRNA expression was inhibited after treatment with LNP-Vig nanoparticles, indicating that LNP-Vig negatively regulates EGFR expression. On the basis of LNP-Vig treatment, after transfection with si-EGFR, the expression of EGFR mRNA was greatly reduced, which further enhanced the inhibitory effect on EGFR, indicating that the intervention of si-EGFR can effectively reduce the expression level of EGFR. In addition, the expression of EGFR protein was also significantly increased in the pc-DNA EGFR treatment group, indicating that the up-regulation of pc-DNA EGFR enhanced the protein expression of EGFR. The EGFR and NOTCH1 pathways cross-regulate each other in many biological processes, forming complex signaling networks. After the EGFR pathway is activated, the activity of the NOTCH1 pathway can be promoted by activating a series of downstream signaling molecules and transcription factors (Wang *et al*., 2024).

In the active state, the NOTCH1 receptor is cleaved to produce an active inner cytoplasmic domain, which then enters the nucleus, binds to transcription factors, regulates the transcription of specific genes and affects biological processes such as cell growth, proliferation, differentiation and stem cell maintenance. Activation of the EGFR pathway may inhibit the NOTCH1 pathway, or the activity of the NOTCH1 pathway may affect the EGFR pathway (Sweed *et al*., 2024). When the NOTCH1 pathway is inhibited, the active NOTCH1 receptor cannot be activated or transcription factors cannot bind to it, resulting in the inhibition of Hes1 expression (Xie *et al*., 2025). Therefore, the decreased level of Hes1 protein may affect the biological function of cells. Further treatment with LNP-PV in the experiments inhibited the EGFR pathway and also resulted in consistent negative regulation of downstream NOTCH1 and Hes1 gene expression. This indicated that LNP-Vig may regulate the expression of NOTCH1 pathway and Hes1 gene by inhibiting EGFR pathway. Hes1 is the main downstream effector molecule of the NOTCH1 pathway. When the NOTCH1 pathway is activated, the expression level of Hes1 gene will be up-regulated, leading to an increase in the expression of Hes1 protein. As a transcriptional repressor, Hes1 protein can inhibit the transcription of some genes related to cell cycle and apoptosis, including some genes related to cell cycle and apoptosis and prevent the process of cell death. Conversely, inhibition of the Hes1 gene reduces Hes1 protein levels, which may upregulate pro-apoptotic genes, promote glioma cell apoptosis and subsequently activate ferroptosis (Paskeh *et al*., 2024). Therefore, it is speculated that the mechanism by which LNP-PV activates ferroptosis may involve inhibition of the EGFR pathway, thereby affecting the expression of the NOTCH1 pathway and the Hes1 gene. The regulation of NOTCH1 pathway and Hes1 gene may be the downstream events of ferroptosis activated by LNP-Vig.

For the treatment of glioma, promoting the ferroptosis of glioma cells may become a new therapeutic strategy. By regulating the level of intracellular iron ions or increasing the degree of oxidative stress, it may promote the self-destruction of glioma cells, so as to achieve the therapeutic effect (Tran *et al*., 2023). After a specific γ-secretase blocker of the NOTCH1 pathway was further used, the

levels of ferroptosis-related proteins in the LNP-PV group decreased, indicating that the NOTCH1 pathway played an important role in the promotion of ferroptosis by LNP-PV. After using the si-Hes1 group, the expression level of ferroptosis-related proteins decreased, which was consistent with the experimental results of blocking the NOTCH1 pathway, indicating that the Hes1 gene plays an important regulatory role in the activation of ferroptosis by LNP-Vig. In turn, activation of the NOTCH1 pathway or overexpression of Hes1 led to increased expression levels of ferroptosis-related proteins and reversed the ferroptosis-promoting effect of LNP-Vig. Therefore, it was confirmed that LNP-Vig promoted the apoptosis of U87MG cells and activated the process of ferroptosis by regulating the expression of the NOTCH1 pathway and the Hes1 gene. The NOTCH1 pathway and Hes1 gene play a key role in the regulation of ferroptosis by LNP-Vig, which provides a deeper understanding for further revealing the mechanism of ferroptosis activated by LNP-Vig and also provides potential for the development of new strategies in tumor therapy.

Although this study focuses on the role of EGFR pathway and NOTCH1 pathway in LNP-Vig-activated ferroptosis, other mechanisms may be involved. Other potential signaling pathways and regulators have not been comprehensively studied, which may lead to an incomplete understanding of the mechanism of ferroptosis. However, this study has several limitations. The limited sample size used may introduce bias into the results. Furthermore, the experiments were conducted solely in the U87MG cell line; the generalizability of this pathway has not been verified in other glioma cell lines (e.g., U251, LN229) or primary tumor cells, which is a critical safety issue that must be addressed before clinical translation. Moreover, all conclusions are based on in vitro experiments, lacking validation at the animal model level (*in-vivo*). Therefore, future research should further validate the anti-tumor efficacy of LNP-Vig in various glioma models and *in vivo* settings; systematically assess its toxicity to normal neural cells and the selective index to ensure therapeutic safety; and explore the synergistic effects of LNP-Vig with other standard therapies, such as temozolomide.

CONCLUSION

In summary, this study successfully prepared LNP-Vig nanoparticles and demonstrated their ability to promote ferroptosis in U87MG glioma cells by inhibiting the EGFR/NOTCH1/Hes1 signaling pathway. LNP-Vig exhibited favorable biocompatibility and pro-apoptotic effects, mechanisms that are closely associated with ROS accumulation and the regulation of iron metabolism. Future research should focus on further *in vivo* experiments and validation across multiple cancer types to advance its clinical translation.

Acknowledgments
We gratefully acknowledge the First Medical Center of Chinese PLA General Hospital Laboratory for providing the necessary equipment for this study.

Authors' contributions
Zhao Gao and Shichao Su: Conceived and designed the study and drafted the manuscript; Yuxin Wang and Jiayu Liu: Collected, analyzed and interpreted the experimental data. All authors revised the manuscript for important intellectual content. All authors read and approved the final manuscript. It is declared that this work was done by the authors named in this article and all liabilities pertaining to claims relating to the content of this article will be borne by the authors.

Funding
There was no funding.

Data availability statement
Data are available from the corresponding author.

Ethical approval
This study was approved by the Ethics Committee of Chinese PLA General Hospital (Approval No.: S2022-763-01).

Conflict of interest
The authors declare that the research was conducted in the absence of any commercial or financial relationships that could be construed as a potential conflict of interest.

REFERENCES

Agunloye MO, Owu DU, Onaadepo O, Bisong SA, Ogunyemi OM and Ugwu FN (2025). The role of avocado plant and its derivatives in the management of diabetes mellitus: A natural approach to glycemic control. *J Diabetes Metab Disord*., **24**(1): 34.

Bode K, Link C, Krammer PH and Weyd H (2020). Flow-cytometric detection of low-level reactive oxygen species in cell lines and primary immune cells. *Bio Protoc*, **10**(17): e3737.

Bu X and Wang L (2025). Iron metabolism and the tumor microenvironment: A new perspective on cancer intervention and therapy (Review). *Int J Mol Med*., **55**(3): 39.

Chen Y, Guo X, Zeng Y, Mo X, Hong S, He H, Li J, Fatima S and Liu Q (2023). Oxidative stress induces mitochondrial iron overload and ferroptotic cell death. *Sci. Rep*., **13**(1): 15515.

Das M, Joshi A, Devkar R, Seshadri S and Thakore S (2022). Vitamin-H channeled self-therapeutic P-gp inhibitor curcumin-derived nanomicelles for targeting the tumor milieu by pH- and enzyme-triggered hierarchical disassembly. *Bioconjug Chem*., **33**(2): 369–385.

Del Re DP, Matsuda T, Zhai PY, Maejima Y, Jain MR, Liu T, Li H, Hsu CP and Sadoshima J (2014). Mst1 promotes cardiac myocyte apoptosis through phosphorylation and inhibition of Bcl-xL. *Molecular Cell*, **54**(4): 639-650.

Ding Y, Xiang Q, Zhu P, Fan M, Tong H, Wang M, Cheng S, Yu P, Shi H, Zhang H and Chen X (2024). Qihuang Zhuyu formula alleviates coronary micro thrombosis by inhibiting PI3K/Akt/αIIbβ3-mediated platelet activation. *Phytomedicine*., **125**: 155276.

Dong J, Guo H, Yang R, Li H, Wang S, Zhang J and Chen W (2011). Serum LDL- and HDL-cholesterol determined by ultracentrifugation and HPLC. *J Lipid Res*, **52**(2): 383-388.

Fan X, Li A, Yan Z, Geng X, Lian L, Lv H, Gao D and Zhang J (2022). From iron metabolism to ferroptosis: Pathologic changes in coronary heart disease. *Oxid Med Cell Longev*., **2022**: 6291889.

Husain K, Coppola D, Yang CS and Malafa MP (2024). Effect of vitamin E δ-tocotrienol and aspirin on Wnt signaling in human colon cancer stem cells and in adenoma development in APCmin/+ mice. *Carcinogenesis*, **45**(12): 881–892.

Iervolino M, Lepore E, Forte G, Lagana AS, Buzzaccarini G and Unfer V (2021). Natural molecules in the management of polycystic ovary syndrome (PCOS): An analytical review. *Nutrients*, **13**(5): 1677.

Imbastari F, Dahlmann M, Sporbert A, Mattioli CC, Mari T, Scholz F, Timm L, Twamley S, Migotti R, Walther W, Dittmar G, Rehm A and Stein U (2021). MACC1 regulates clathrin-mediated endocytosis and receptor recycling of transferrin receptor and EGFR in colorectal cancer. *Cell Mol Life Sci.,* **78**(7): 3525–3542.

Jiang Y, Zhao J, Li R, Liu Y, Zhou L, Wang C, Lv C, Gao L and Cui D (2022). CircLRFN5 inhibits the progression of glioblastoma via PRRX2/GCH1 mediated ferroptosis. *J Exp Clin Cancer Res.,* **41**(1): 307.

Le X and Fan YF (2023). ADAM17 regulates the proliferation and extracellular matrix of keloid fibroblasts by mediating the EGFR/ERK signaling pathway. *J Plast Surg Hand Surg*., **57**(1-6): 129–136.

Liang W and Ferrara N (2021). Iron metabolism in the tumor microenvironment: Contributions of Innate Immune Cells. *Front Immunol*., **11**: 626812.

Livak KJ and Schmittgen TD (2001). Analysis of relative gene expression data using real-time quantitative PCR and the 2(-Delta Delta C(T)) Method. *Methods*, **25**(4): 402-408.

Lu S, Wang XZ, He C, Wang L, Liang SP, Wang CC, Li C, Luo TF, Feng CS, Wang ZC, Chi GF and Ge PF (2021). ATF3 contributes to brucine-triggered glioma cell ferroptosis via promotion of hydrogen peroxide and iron. *Acta Pharmacol Sin*., **42**(10): 1690–1702.

McClements DJ and Ozturk B (2022). Utilization of nanotechnology to improve the application and bioavailability of phytochemicals derived from waste streams. *J. Agric. Food Chem*., **70**(23): 6884–6900.

Mijiti M, Maimaiti A, Chen X, Tuersun M, Dilixiati M, Dilixiati Y, Zhu G, Wu H, Li Y, Turhon M, Abulaiti A, Maimaitiaili N, Yiming N, Kasimu M and Wang Y (2023). CRISPR-cas9 screening identified lethal genes enriched in Hippo kinase pathway and of predictive significance in primary low-grade glioma. *Mol Med*., **29**(1): 64.

Nag S, Manna K, Saha M and Das Saha K (2020). Tannic acid and vitamin E loaded PLGA nanoparticles ameliorate hepatic injury in a chronic alcoholic liver damage model via EGFR-AKT-STAT3 pathway. *Nanomedicine (Lond).,* **15**(3): 235–257.

Paskeh MDA, Babaei N, Hashemi M, Doosti A, Hushmandi K, Entezari M and Samarghandian S (2024). The protective impact of curcumin, vitamin D and E along with manganese oxide and Iron (III) oxide nanoparticles in rats with scrotal hyperthermia: Role of apoptotic genes, miRNA and circRNA. *J Trace Elem Med Biol*., **81**: 127320.

Rochette L, Dogon G, Rigal E, Zeller M, Cottin Y and Vergely C (2022). Lipid peroxidation and iron Metabolism: Two corner stones in the homeostasis control of ferroptosis. *Int J Mol Sci*., **24**(1): 449.

Sacco A, Battaglia AM, Botta C, Aversa I, Mancuso S, Costanzo F and Biamonte F (2021). Iron metabolism in the tumor microenvironment-implications for anti-cancer immune response., *Cell*. **10**(2): 303.

Seidu TA, Kutoka PT, Asante DO, Farooq MA, Alolga RN and Bo W (2022). Functionalization of nanoparticulate drug delivery systems and its influence in cancer therapy. *Pharmaceutics*., **14**(5): 1113.

Stockwell BR (2022). Ferroptosis turns 10: Emerging mechanisms, physiological functions and therapeutic applications. *Cell*., **185**(14): 2401–2421.

Sweed NM, Zaafan MA, El-Bishbishy MH and Dawoud MHS (2024). The pulmonary protective potential of vanillic acid-loaded TPGS-liposomes: Modulation of miR-217/MAPK/NF-κb signalling pathway. *J Microencapsul*., **41**(4): 255–268.

Tabu K and Taga T (2022). Cancer ego-system in glioma: An iron-replenishing niche network systemically self-organized by cancer stem cells. *Inflamm. Regen.,* **42**(1): 54.

Tran NH, Ryzhov V, Volnitskiy A, Amerkanov D, Pack F, Golubev AM, Arutyunyan A, Spitsyna A, Burdakov V, Lebedev D, Konevega AL, Shtam T and Marchenko Y (2023). Radiosensitizing effect of dextran-coated iron oxide nanoparticles on malignant glioma cells. *Int J Mol Sci*., **24**(20): 15150.

Vesely O, Baldovska S and Kolesarova A (2021). Enhancing bioavailability of nutraceutically used resveratrol and other stilbenoids. *Nutrients*., **13**(9): 3095.

Wang S, Zhang Y, Zhong Y, Xue Y, Liu Z, Wang C, Kang DD, Li H, Hou X, Tian M, Cao D, Wang L, Guo K, Deng B, McComb DW, Merad M, Brown BD and Dong Y (2024). Accelerating diabetic wound healing by ROS-scavenging lipid nanoparticle-mRNA formulation. *Proc Natl Acad Sci U S A*., **121**(22): e2322935121.

Wang Y, Wang X, Wang K, Qi J, Zhang Y, Wang X, Zhang L, Zhou Y, Gu L, Yu R and Zhou X (2023). Chronic stress accelerates glioblastoma progression via DRD2/ERK/β-catenin axis and Dopamine/ERK/TH positive feedback loop. *J Exp Clin Cancer Res*., **42**(1): 161.

Wu X, Ueland PM, Roper J, Koh GY, Liang X, Crott JW, Yilmaz ÖH, Bronson RT and Mason JB (2021). Combined supplementation with vitamin B-6 and curcumin is superior to either agent alone in suppressing obesity-promoted colorectal tumorigenesis in mice. *J. Nutr*., **151**(12): 3678–3688.

Xie Q, He Z, Tan L, Li M, Zhuang M, Liu C, Chen S, Jin L and Sui Y (2025). Hesperetin induces apoptosis in lung squamous carcinoma cells via G2/M cycle arrest, inhibition of the Notch1 pathway and activation of endoplasmic reticulum stress. *Int J Mol Med*., **55**(5): 77.

Yathindranath V, Safa N, Sajesh BV, Schwinghamer K, Vanan MI, Bux R, Sitar DS, Pitz M, Siahaan TJ and Miller DW (2022). Spermidine/spermine N1-acetyltransferase 1 (SAT1)-A potential gene target for selective sensitization of glioblastoma cells using an ionizable lipid nanoparticle to deliver siRNA. *Cancers (Basel)*., **14**(21): 5179.

Yasinjan F, Xing Y, Geng H, Guo R, Yang L, Liu Z and Wang H (2023). Immunotherapy: A promising approach for glioma treatment. *Front Immunol*., **14**: 1255611.

Ye D, Zhang Y, Zhang B, Liu J, Wei T and Lu S (2024). The regulatory role of m6A methylation modification in metabolic syndrome pathogenesis and progression. *Front Physiol*., **15**: 1271874.

Yu H, Zhu K, Wang M and Jiang X (2023). TXNDC12 knockdown promotes ferroptosis by modulating SLC7A11 expression in glioma. *Clin Transl Sci*., **16**(10): 1957-1971.

Zhang P, Rashidi A, Zhao J, Silvers C, Wang H, Castro B, Ellingwood A, Han Y, Lopez-Rosas A, Zannikou M, Dmello C, Levine R, Xiao T, Cordero A, Sonabend AM, Balyasnikova IV, Lee-Chang C, Miska J and Lesniak MS (2023). STING agonist-loaded, CD47/PD-L1-targeting nanoparticles potentiate antitumor immunity and radiotherapy for glioblastoma. *Nat Commun*., **14**(1): 1610.

Zhang D, Duque-Jimenez J, Facchinetti F, Brixi G, Rhee K, Feng WW, Janne PA and Zhou X (2025). Transferrin receptor targeting chimeras for membrane protein degradation. *Nature*., **638**(8051): 787–795.